J. Electrochem. Sci. Eng. **12(6)** (2022) 1251-1259; http://dx.doi.org/10.5599/jese.1375

Open Access : : ISSN 1847-9286
www.jESE-online.org

Original scientific paper

A WSe_2@poly(3,4-ethylenedioxythiophene) nanocomposite-based electrochemical sensor for simultaneous detection of dopamine and uric acid

Yasin Tangal[1], Deniz Coban[2] and Sadik Cogal[3,✉]

[1]*Burdur Mehmet Akif Ersoy University, The Graduate School of Natural and Applied Sciences, Department of Chemistry, 15030, Burdur, Turkey*
[2]*Burdur Mehmet Akif Ersoy University, The Graduate School of Natural and Applied Sciences, Department of Material Technology Engineering, 15030, Burdur, Turkey*
[3]*Burdur Mehmet Akif Ersoy University, Faculty of Arts and Science, Department of Chemistry, 15030, Burdur, Turkey*

Corresponding author: ✉*sadik_cogal@yahoo.com; Tel.: +90-248-213-3060; Fax: +90-248-213-3099*

Received: May 13, 2022; Accepted: June 24, 2022; Published: July 25, 2022

Abstract

In the present work, a nanocomposite of two-dimensional WSe_2 nanosheets with poly-(3,4-ethylenedioxythiophene (WSe_2@PEDOT) was prepared by facile hydrothermal method and characterized in terms of structural and morphological analyses. This nanocomposite was used to modify glassy carbon electrode for the construction of an electrochemical sensing platform for simultaneous determination of dopamine (DA) and uric acid (UA) in the presence of ascorbic acid (AA). It was found that the incorporation of PEDOT into WSe_2 nanosheets exhibited enhanced electrochemical behaviors and electro¬catalytic activity against DA and UA. Using differential pulse voltammetry (DPV) measurements, the WSe_2@PEDOT modified electrode displayed wide linear detection ranges of 16 to 466 µM for DA and 20 to 582.5 µM for UA. The electrode also exhibited high selectivity against DA and UA in the presence of major interference of ascorbic acid and other interferent substances.

Keywords

Tungsten diselenide; conducting polymer; modified electrode; selective sensing; biological compounds

Introduction

Dopamine (DA) and uric acid (UA) are two important biological compounds that play important roles in human physiological functions [1]. Abnormal concentrations of these molecules in biological fluids lead to many diseases, including schizophrenia, Alzheimer, Parkinson's disease, drug addiction, hyperuricemia, chronic renal sickness, *etc.* [2-4]. Therefore, early analyses of these molecules are highly important to deal with the concerned conditions. Recently, electrochemical methods have

become attractive for the determination of DA and UA [5,6]. However, these two electroactive molecules have close oxidation potentials, which limits their selective detection in biological samples on traditional electrodes. Therefore, tremendous research efforts have been directed toward the development of novel electrodes based on various materials. Among these, two-dimensional (2D) nanomaterials such as graphene and its inorganic analogues have attracted significant interest in electrochemical applications because of their unique chemical and physical properties [7]. For example, transition metal dichalcogenides (TMDs) have been widely investigated as electrode materials for electrochemical sensing platforms due to their high electrocatalytic properties, chemical stability, low cost and facile synthesis [8-10]. WSe_2, an important member of TMDs, has received special attention in electrochemical applications [11,12]. However, WSe_2 tends to stack easily due to high interactions between its layers, which decrease the number of electroactive sites and electrochemical performance. Therefore, various strategies have been applied to improve the electrochemical performance to decrease the number of layers and enhance the number of active sites. Among the alternative strategies, the production of WSe_2 in the presence of conductive supports is an effective way to reduce the number of layers by preventing layer stacking. Conducting polymers such as poly(3,4-ethylenedioxythiophene) (PEDOT) can be incorporated with TMD materials to prepare composite electrode materials [13,14]. PEDOT possesses high conductivity and electrochemical stability and shows high potential to be applied to an electrode material [15]. PEDOT- like supporting materials not only prevent the stacking of WSe_2 layers but also increase the active sites of WSe_2.

In this work, WSe_2@PEDOT composite was prepared *via* a hydrothermal method to enhance the electrochemical properties of WSe_2. The as-prepared composite was coated on a glassy carbon electrode (GCE) for electrochemical detection of DA and UA.

Experimental

Materials: Tungstic acid (H_2WO_4) (Aldrich, 99 %), selenium (Se) powder (Sigma-Aldrich, 99.0 %), sodium borohydride ($NaBH_4$) (Sigma-Aldrich, ≥98 %), 3,4-ethylenedioxythiophene (EDOT) (Sigma-Aldrich, 97 %), iron (III) chloride ($FeCl_3$) (Carlo Erba), potassium chloride (Sigma-Aldrich), potassium ferricyanide(III) ($K_3Fe(CN)_6$) (Sigma-Aldrich, 99 %), potassium hexacyanoferrate(II) trihydrate ($K_4[Fe(CN)_6]\cdot 3H_2O$) (Merck), sodium phosphate monobasic dihydrate ($NaH_2PO_4\cdot 2H_2O$) (Sigma-Aldrich), sodium phosphate dibasic dihydrate ($Na_2HPO_4\cdot 2H_2O$) (Sigma-Aldrich) and dimethylformamide (DMF) (Merck) were purchased and used as received.

Synthesis of PEDOT: PEDOT was synthesized *via* the oxidative chemical polymerization method. 100 µL of monomer EDOT was dissolved in 50 mL deionized water (DIW) and placed in an ice bath. In another flask, 422.9 mg ammonium persulfate (APS) (EDOT:APS molar ratio is 1:2) was dissolved in 25 mL DIW and then transferred slowly to monomer solution, keeping the temperature of the solution between 0-5 °C. The reaction mixture was stirred for 48 h at room temperature. The obtained black powder was filtered, washed with DIW and ethanol several times and finally dried at 60 °C for 24 h.

Synthesis of WSe_2@PEDOT

*T*he preparation of WSe_2@PEDOT was carried out as follows: first, 0.1 g of as-prepared PEDOT was ultrasonically dispersed in 30 mL of DMF for 60 min. Then, 0.32 g Se powder and 0.1 g $NaBH_4$ as a reducing agent were added and stirred for 60 min to obtain good dispersion. Later, 0.49 g H_2WO_4 was slowly added to this dispersion and stirred for an additional 30 min. The final dispersion was transferred to a 45 mL Teflon-lined stainless steel autoclave reactor and heated at 200 °C for 12 h. After being cooled to room temperature, the product was filtered and washed with DW at

least three times and finally dried at 60 °C. The obtained powder was annealed at 500 °C for 3 h under N_2 flow to enhance the crystallinity.

The synthesis of WSe_2 as control was the same as that of WSe_2@PEDOT, except PEDOT was not added to the reaction mixture.

Electrode modification

Before coating, the cleaning process was applied to polish the GCE surface by using 0.3 and 0.05 µm alumina powder. GCE was then sonicated in DW and ethanol to remove any adsorbed particles on its surface. On the other hand, well-dispersed electrode ink was prepared by sonication of WSe_2@PEDOT in DMF for 1 h to obtain a concentration of 5 mg mL^{-1} WSe_2@PEDOT. Later, 10 µL from this ink was drop-coated on GCE and left to dry in an open atmosphere. Finally, WSe_2@PEDOT coated-GCE was carefully rinsed with 0.1 M phosphate buffer solution (PBS) before experiments.

For the control, GCE was also modified with pristine WSe_2 in the same way described above for GCE/WSe_2@PEDOT.

Electrochemical measurements

Electrochemical experiments were conducted *via* Ivium CompactStat model potentiostat. Three-electrode configuration was used for electrochemical works, and in addition to GCE as a working electrode, Pt wire was used as a counter electrode and Ag/AgCl as a reference electrode.

Characterization

The crystal structure of the as-prepared WSe_2@PEDOT was determined through X-ray diffraction (XRD) using Bruker/D8 Advance diffractometer. Morphological characterization was conducted using scanning electron microscopy (FEI Model: Quanta 400F) and transmission electron microscopy (FEI Tecnai G2 Spirit Biotwin model).

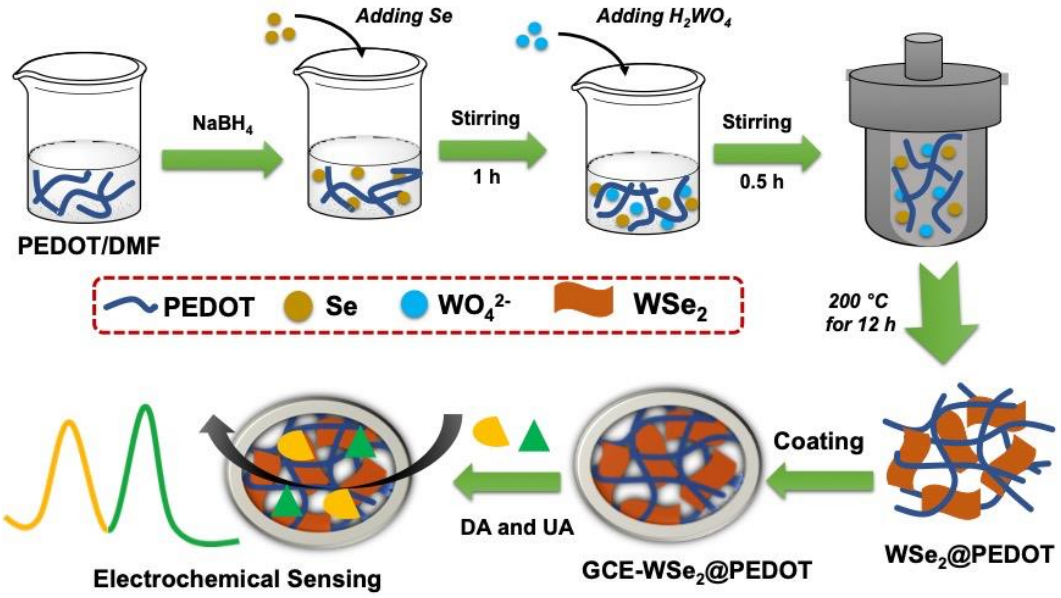

Figure 1. *Schematic representation of synthetic procedure and electrochemical detection*

Results and discussion

Materials characterization

WSe_2@PEDOT composite was successfully obtained *via* hydrothermal reaction, as schematically represented in Figure 1. In this synthesis procedure, metallic Se particles were initially reduced by a

reducing agent of $NaBH_4$ to produce Se^{2-} ions. The Se^{2-} ions were then reacted with W cations, forming WSe_2 nanosheets embedded in PEDOT polymeric structure.

The structure of the WSe_2@PEDOT composite was evaluated by X-ray diffraction (XRD). Figure 2 shows the XRD patterns of the WSe_2@PEDOT composite as well as pristine WSe_2 nanosheets. XRD pattern of WSe_2 displays major diffraction peaks (planes) at 13.3° (002), 31.9° (100), 37.6° (103), 47.3° (105), 55.9° (110), 65.8° (108) and 70.3° (203), which are in good agreement with the well-known hexagonal WSe_2 structure (JCPDS No. 38-1388) [16]. On the other hand, the WSe_2@PEDOT composite exhibited diffraction peaks at 13.2, 23.0, 31.4, 32.8, 37.8, 40.6, 47.3, 53.3, 55.9, 65.7, 69.4 and 74.2°, in which the major diffraction peaks of WSe_2 hexagonal structure are well matched. Moreover, the major diffraction peaks are relatively stronger, and additional diffraction peaks are also observed in the WSe_2@PEDOT composite, suggesting the successful combination of WSe_2 nanosheets and conducting polymer.

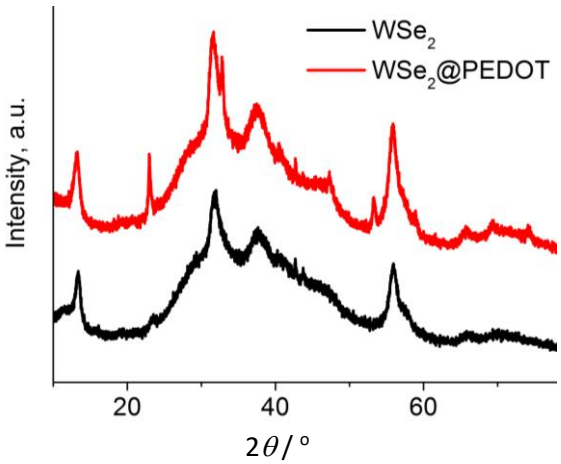

Figure 2. *XRD pattern of WSe_2 nanosheets and WSe_2@PEDOT composite*

The surface morphology of the WSe_2@PEDOT composite was investigated using SEM and TEM. The SEM images (Figure 3a-b) of pristine WSe_2 and WSe_2@PEDOT indicate that nanosheets incorporated flower-like structures were obtained by hydrothermal treatment. However, the WSe_2@PEDOT possesses looser, dispersed and thinner nanosheets due to the incorporation of PEDOT. This difference is more obvious in the TEM images, as shown in Figure 3c-d. Thus, the resulting composite can have more active sites for analyte adsorption, leading to an improved electrochemical signal.

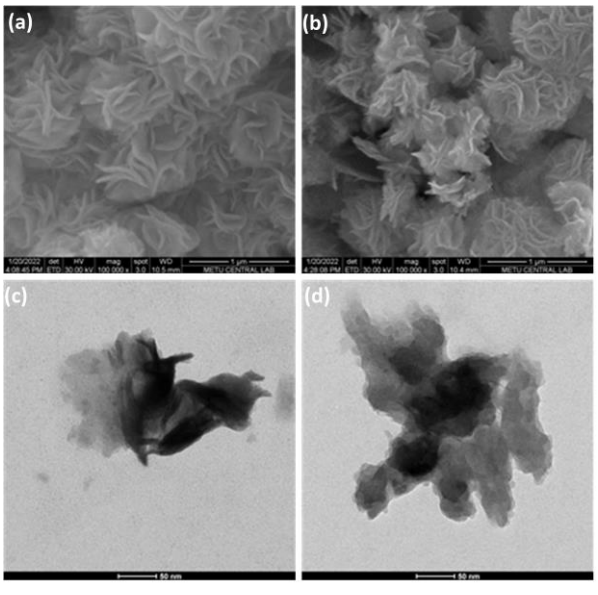

Figure 3. *(a,b) SEM and (c,d) TEM images of WSe_2 (left) and WSe_2@PEDOT (right)*

Electrochemical studies

To assess the electrochemical behavior, modified electrodes were investigated *via* cyclic voltammetry (CV) in 0.1 M KCl containing 5 mM $[Fe(CN)_6]^{3-/4-}$, conducted between -0.3 to 0.6 V at 50 mV s^{-1} of scan rate (ν). Figure 4(a) shows CVs of bare GCE, GCE-WSe_2 and GCE-WSe_2@PEDOT in this solution. It is obvious that the WSe_2@PEDOT composite-modified electrode exhibited better electrochemical kinetics against ferri/ferrocyanide couple than bare GCE and GCE-WSe_2. WSe_2@PEDOT displays 99.1 / -106.1 µA of anodic/cathodic peak currents, while the bare GCE and GCE-WSe_2 show 51.2 / -60.1 µA and 75.01 / -86.3 µA, respectively. The enhanced electrochemical kinetics of GCE-WSe_2@PEDOT could be attributed to the enhanced number of electroactive sites and higher conductivity due to the incorporation of conductive PEDOT in WSe_2 nanosheets.

To estimate the electrochemically active surface area of the GCE-WSe_2@PEDOT electrode, CV measurements at various scan rates were performed in 0.1 M KCl containing 5 mM $[Fe(CN)_6]^{3-/4-}$ (Figure 4b). The inset figure shows that the anodic peak currents increased linearly with the square root of scan rates ($\nu^{1/2}$). Therefore, the electrochemically active surface area (A / cm^2) was calculated using Randles-Ševčik equation (1) [17]:

$$I_{pa} = (2.65 \times 10^5)\, n^{3/2} A D^{1/2} C \nu^{1/2} \qquad (1)$$

where D is the diffusion coefficient, which is 7.6×10^{-6} cm^2 s^{-1} for $[Fe(CN)_6]^{3-/4-}$. The electrochemical surface area of the GCE-WSe_2@PEDOT electrode was estimated to be 0.13 cm^2, which is higher than 0.063 cm^2 estimated for bare GCE.

In order to determine the electrocatalytic activities of bare, WSe_2 and WSe_2@PEDOT modified electrodes toward a binary mixture of DA and UA, the CV and DPV measurements were performed in 0.1 M PBS solution containing 0.19 mM DA and 0.28 mM UA. Figure 4c shows CVs of different electrodes performed in the potential range between -0.2 to +0.6 V, at 50 mV/s of scan rate. It is clearly seen that the current response of bare GCE is very low, which does not provide a sensitive sensing system for the determination of DA and UA. On the other hand, as it is expected by modifying the GCE electrode, the current response was improved and the highest activity was obtained with the electrode modified with WSe_2@PEDOT composite.

Electrocatalytic activities of electrodes were further investigated using the DPV technique, which is known as a more sensitive electrochemical method. Figure 4d shows that oxidation peak positions and their current responses are more obvious than was observed in CV measurements. Therefore, the DPV technique was chosen for the simultaneous determination of DA and UA. Moreover, from the CV and DPV curves, it is obviously seen that the current response of UA was greatly increased. This enhancement of the WSe_2@PEDOT modified electrode toward UA is due to the presence of PEDOT conducting polymer. At the working pH, DA has a cationic character and UA exists as an anionic form, which leads to enhanced electrostatic interaction between UA and cationic PEDOT [18]. Therefore, different interactions of DA and UA with the WSe_2@PEDOT composite result in peak separation of DA and UA.

Cyclic voltammetry was also used to evaluate the effect of various scan rates on the electrocatalytic behaviors of DA and UA on the WSe_2@PEDOT electrode and to understand the reaction kinetics on its surface. Figure 5(a) displays CVs of DA (0.28 mM) and UA (0.37 mM) in 0.1 M PBS at varied scan rates from 25 to 250 mV/s. Figure 5b shows the corresponding oxidation peak currents, which are proportional to the scan rate, indicating an adsorption-controlled process on WSe_2@PEDOT coated electrode [19].

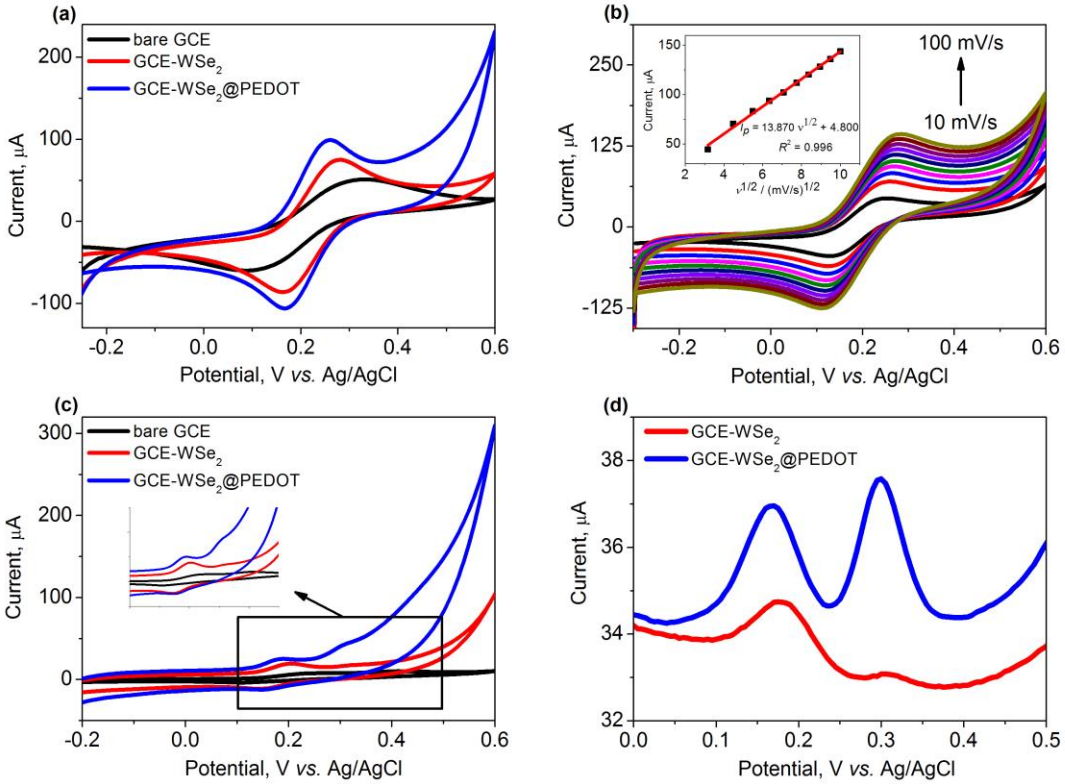

Figure 4. *(a) CVs of GCE, GCE-WSe$_2$ and GCE-WSe$_2$@PEDOT in 0.1 M KCl containing 5 mM $[Fe(CN)_6]^{3-/4-}$; (b) CVs of GCE-WSe$_2$@PEDOT in 0.1 M KCl containing 5 mM $[Fe(CN)_6]^{3-/4-}$ at different scan rates; Inset figure shows anodic peak currents vs. square roots of scan rates; (c) CVs of GCE, GCE-WSe$_2$ and GCE-WSe$_2$@PEDOT in 0.1 M PBS solution containing 0.19 mM DA and 0.28 mM UA; (d) DPVs of GCE-WSe$_2$ and GCE-WSe$_2$@PEDOT in 0.1 M PBS solution containing 0.19 mM DA and 0.28 mM UA*

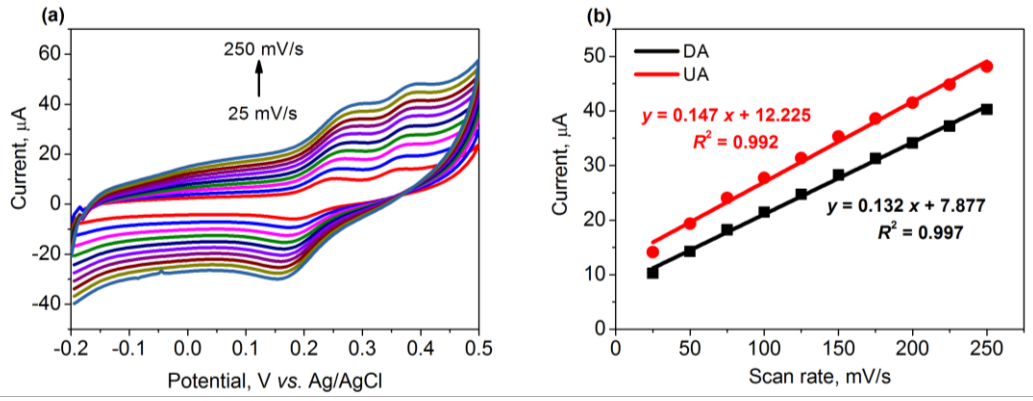

Figure 5. *(a) CVs of GCE-WSe$_2$@PEDOT in 0.1 M PBS (pH 7.0) containing 1.5 mM AA, 0.36 mM DA and 0.55 mM UA at different scan rates from 25-25 mV/s; (b) linear plots of anodic peak currents of DA and UA vs. scan rate*

The simultaneous determination of DA and UA on GCE-WSe$_2$@PEDOT was performed using DPV. Figure 6a displays the DPVs for increasing DA and UA concentrations in 0.1 M PBS. It is obvious that oxidation peak positions of DA and UA maintain the peak-to-peak potential separation by gradually increasing their concentrations. Figure 6(b-c) displays calibration curves of DA and UA and linear detection ranges of 16 to 466 µM for DA and 20 to 582.5 µM for UA, were determined. The linear regression equations with corresponding regression coefficients were also placed in Figure 6b, c. Furthermore, considering the slopes of the regression equations, LODs were evaluated to be 8 µM for DA and 14 µM UA, respectively.

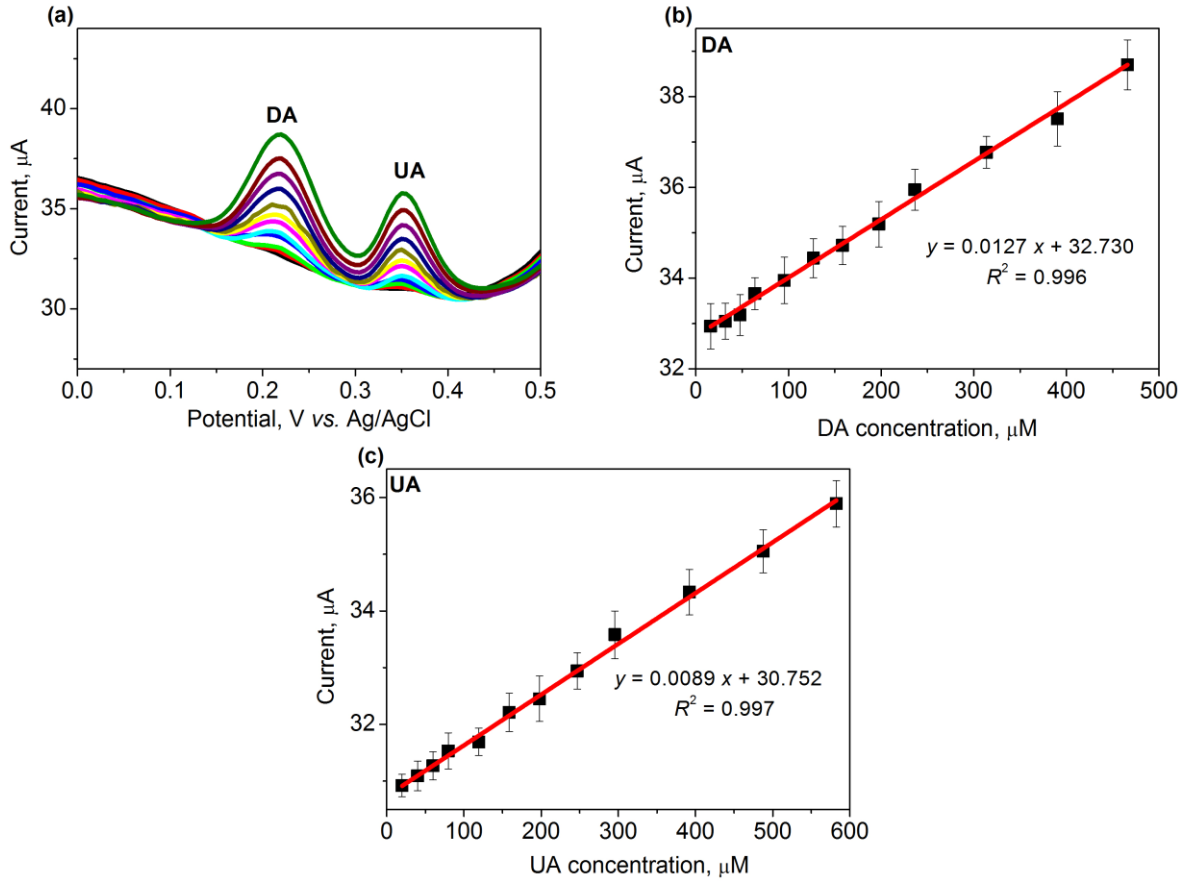

Figure 6. *(a) DPVs of GCE-WSe_2@PEDOT in 0.1 M PBS (pH 7.0) containing various concentrations of DA and UA; calibration plots of (b) DA and (c) UA*

Selectivity, reproducibility and stability of the sensor

The selectivity of the GCE-WSe_2@PEDOT electrode was investigated through DPV technique. The major interference molecule is ascorbic acid, found in a much higher concentration than DA and UA in biological fluids. Figure 7a shows DPVs of GCE-WSe_2@PEDOT in 0.1 M PBS solution containing 0.38 mM DA, 0.38 mM UA and 1.0 mM AA and other interference substances (*e.g.*, NaCl, KCl, $NaNO_3$, $MgSO_4$, glucose and citric acid).

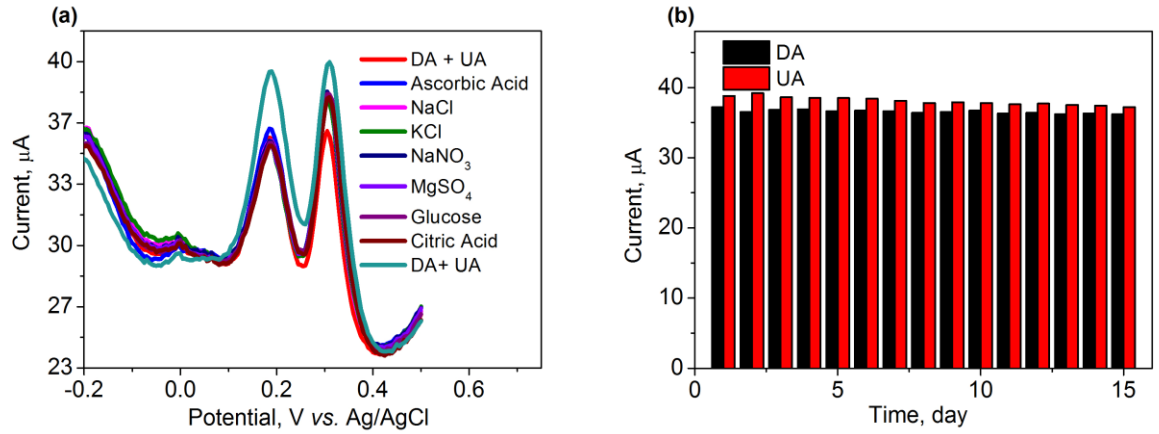

Figure 7. *(a) DPVs of GCE-WSe_2@PEDOT in 0.1 M PBS (pH 6.0) containing 1.0 mM interfering substances in presence of 0.38 mM DA and 0.38 mM UA; (b) stability test*

It is clearly seen that adding interfering substances in much higher concentrations to the mixed DA and UA solution does not have an obvious change in their peak currents, indicating high selectivity of

the sensor. It is also worth noting that the electrode modified with WSe_2@PEDOT inhibits the oxidation of AA, which has a close oxidation potential to DA and UA. The stability test of the GCE-WSe_2@PEDOT electrode was also investigated using the DPV technique. The stability data was collected by obtaining the peak current values of DA and UA for fifteen days and given in Figure 7b, indicating an acceptable change compared with the initial currents.

Conclusions

WSe_2@PEDOT composite was successfully prepared *via* a simple hydrothermal method and applied as an electrochemical sensor for the detection of DA and UA. It was found that the incorporation of conducting PEDOT polymer into the WSe_2 nanostructure improved electrochemical behavior and electrocatalytic activity of composite material. Furthermore, WSe_2@PEDOT modified electrode gave separated oxidation peaks for DA and UA with better current responses. WSe_2@PEDOT-based sensor exhibited a linear detection range of 16 to 466 µM for DA and 20 to 582.5 µM for UA and detection limits of 8 µM for DA and 14 µM UA, respectively. The selectivity and stability of the modified electrode were also studied through DPV measurements, exhibiting high selectivity in the presence of various interferents and high stability.

References

[1] Z.-H. Sheng, X.-Q. Zheng, J.-Y. Xu, W.-J. Bao, F.-B. Wang, X.-H. Xia, *Biosensors and Bioelectronics* **34 (1)** (2012) 125-131. https://doi.org/10.1016/j.bios.2012.01.030

[2] R. M. Wightman, L. J. May, A. C. Michael, *Analytical Chemistry* **60(13)** (1988) 769A-779A. https://doi.org/10.1021/ac00164a001

[3] V.S.E. Dutt, H.A. Mottola, *Analytical Chemistry* **46(12)** (1974) 1777-1781. https://doi.org/10.1021/ac60348a041

[4] G. Di Chiara, V. Bassareo, S. Fenu, M. A. De Luca, L. Spina, C. Cadoni, E. Acquas, E. Carboni, V. Valentini, D. Lecca, *Neuropharmacology* **47(1)** (2004) 227-241. https://doi.org/10.1016/j.neuropharm.2004.06.032

[5] H. Beitollahi, S. Tajik, M. R. Aflatoonian, A. Makarem *Journal of Electrochemical Science and Engineering* **12** (2022) 199-208. https://doi.org/10.5599/jese.1231

[6] P. Sankaranarayanan, S. V. Venkateswaran, *Journal of Electrochemical Science and Engineering* **10** (2020) 263-279. https://doi.org/10.5599/jese.783

[7] S. Su, J. Chao, D. Pan, L. Wang, C. Fan, *Electroanalysis* **27(5)** (2015) 1062-1072. https://doi.org/10.1002/elan.201400655

[8] R. Sha, N. Vishnu, S. Badhulika, *Sensors and Actuators B* **279** (2019) 53-60. https://doi.org/10.1016/j.snb.2018.09.106

[9] Y. Li, C. Fan, J. Zheng, *Journal of Materials Science: Materials in Electronics* **33(8)** (2022) 5061-5072. https://doi.org/10.1007/s10854-022-07695-y

[10] F. Jiang, W.-S. Zhao, J. Zhang, *Microelectronic Engineering* **225(C)** (2020) 111279. https://doi.org/10.1016/j.mee.2020.111279

[11] Y.-X. Chen, W.-J. Zhang, K.-J. Huang, M. Zheng, Y.-C. Mao, *Analyst* **142(24)** (2017) 4843-4851. https://doi.org/10.1039/C7AN01244F

[12] I. Kim, S. W. Park, D. W. Kim, *Journal of Alloys and Compounds* **827** (2020) 154348. https://doi.org/10.1016/j.jallcom.2020.154348-

[13] Y. Li, H. Lin, H. Peng, R. Qi, C. Luo, *Microchimica Acta* **183(9)** (2016) 2517-2523. https://doi.org/10.1007/s00604-016-1897-1

[14] Y.-J. Huang, M.-S. Fan, C.-T. Li, C.-P. Lee, T.-Y. Chen, R. Vittal, K.-C. Ho. $MoSe_2$, *Electrochimica Acta* **211** (2016) 794-803. https://doi.org/10.1016/j.electacta.2016.06.086

[15] Y. Hui, C. Bian, S. Xia, J. Tong, J. Wang, *Analytica Chimica Acta* **1022** (2018) 1-19. https://doi.org/10.1016/j.aca.2018.02.080
[16] M. Muska, J. Yang, Y. Sun, J. Wang, Y. Wang, Q. Yang. $CoSe_2$, *ACS Applied Nano Materials* **4** (2021) 5796-5807. https://doi.org/10.1021/acsanm.1c00594
[17] W. Gong, J. Li, Z. Chu, D. Yang, S. Subhan, J. Li, M. Huang, H. Zhang, Z. Zhao, *Microchemical Journal* **175** (2022) 107188. https://doi.org/10.1016/j.microc.2022.107188
[18] J. Cheng, X. Wang, T. Nie, L. Yin, S. Wang, Y. Zhao, H. Wu, H. Mei, *Analytical and Bio-analytical Chemistry* **412** (2020) 2433-2441. https://doi.org/10.1007/s00216-020-02455-5
[19] H. Sun, J. Chao, X. Zuo, S. Su, X. Liu, L. Yuwen, C. Fan, L. Wang, *RSC Advances* **4(52)** (2014) 27625-27629. https://doi.org/10.1039/C4RA04046E